MG0414+0534: A DUSTY GRAVITATIONAL LENS

C. R. LAWRENCE[1†], RICHARD ELSTON[2‡], B. T. JANNUZI[3•], AND E. L. TURNER[4••]

[1]Owens Valley Radio Observatory and Palomar Observatory
105-24, California Institute of Technology, Pasadena, CA 91125

[2]Cerro Tololo Inter-American Observatory
Casilla 603, La Serena, Chile

[3]Institute for Advanced Study
Princeton, NJ 08540

[4]Princeton University Observatory
Peyton Hall, Princeton University, Princeton, NJ 80540

ABSTRACT

The gravitational lens system MG 04 14+0534 has an unexceptional four-image lensing geometry; however, the optical counterparts of the radio images are exceedingly red, with spectra unlike that of any previously observed active nucleus. New infrared spectra reveal broad Balmer lines at a redshift of 2.639A 0.002. We use these spectra, in combination with infrared and HST images, IRAS flux densities, the radio images of Hewitt *et* al. (1992) and Katz and Hewitt (1993), and the optical spectrum of Hewitt *et al. (1992),* to argue that the background source in MG 0414+0534 is a typical high-redshift quasar heavily reddened by dust in the lens. Inferred values of visual extinction (A_V) along the path of the brightest image range up to 6 magnitudes, depending on the assumed shape of the unreddened spectrum and the redshift of the lens. Extinction along one of the other image paths is somewhat larger, along the other two somewhat smaller. The image paths all lie roughly 5 kpc from the core of the lens. The presence of large quantities of dust in the lenses of both MG 0414+0534 and MG 1131+ 0456 (Larkin *et al.* 1994) suggests that a significant fraction of massive galaxies at high redshifts is dusty. This has important implications for our understanding of galaxies at high redshift, as well as for optical searches for gravitational lensing.

Subject headings: gravitational lenses - quasars -. radio sources: spectra — galaxies: interstellar matter

1. INTRODUCTION

The gravitational lens system MG 0414-t 0454 has four components in high resolution radio images (Al, A2, B, and C; Hewitt *et al. 1992).* Images in various bands from 5000Å to 9000Å show the same structure, but with different flux ratios. The combined spectrum (Hewitt *et* al. 1992) of A1+A2+B is well-fitted from 4300Å to 9400Å by a power law of $S_\nu \propto \nu^{-8.8}$ or by a black body spectrum with T = 1520 K. There is a strong absorption feature near 8660Å. A near-infrared image by Schechter and Moore (1992) reveals a fifth component, resolved and flattened, within 0.″13 of the position predicted by Hewitt *et al.* for

†crl@jplsp.jpl.nasa.gov. Current address: Astrophysics 169-506, JPL, Pasadena, CA 91109
‡ elston@ctiow2.ctio. noao.edu
•jannuzi@guinness.ias.edu. Hubble Fellow; Visiting Astronomer, KPNO (operated by AURA under contract to the NSF).
•• elt@astro.princeton .edu

the lensing galaxy, and a possible sixth component, as yet unidentified. Images and spectroscopy by Angonin-Willaime *et al. (1994a)* also show the lensing galaxy and the possible sixth component, and show that the optical spectra of components A and B are essentially the same. A deep, wide-field image at 2.2 μm has been obtained by Annis and Luppino (1993).

While there is little doubt that the structure of MG 0414+0454 is due to gravitational lensing, the lensed object itself, based on its observed radio and optical emission, would fit into none of the standard classes of active galactic nuclei. Annis and Luppino (1993) and Angonin-Willaime *et* al. (1994) suggest that the lensed object is a galaxy at high redshift.

In this paper, we describe further observations of this interesting system: 1) images in the J (1.1–1.4 μm), H (1.5- 1.8pm), and K (2.0–2.4 μm) bands; 2) polarimetry in the H band; 3) an HST image in the 702W filter; 4) an IRAS detection of MG 0414+0454 at 60 pm; and 5) spectra covering the *J, H,* and *K* bands.

An intermediate-resolution ($R \sim$ 4000) spectrum of the absorption feature near 8660 Å, obtained with the Keck telescope and given elsewhere in this volume (Lawrence, Cohen, & Oke 1995; hereafter LC095), resolves the feature into four sets of Fe II triplets located near the quasar itself.

From these observations we obtain the redshift of MG 0414+0534, and argue that it is a quasar at high redshift lensed by a massive galaxy with large extinction. If the lens redshift is near the "most likely" value of 0.5 (Kochanek 1992), and the dust is all in the lens, then $4 \lesssim A_V \lesssim 7$ mag along four paths separated by up to 10 kpc in the lens.

2. INFRARED IMAGES AND POLARIMETRY

Infrared images were obtained with the KPNO Infrared Imager (IRIM) and a 58 x 62 InSb array at the $f/8$ Cassegrain focus of the 4 m telescope. Cold fore-optics provided a Lyot stop and produced a final pixel size of 0.″4. Conditions were photometric and the seeing was between 0.″6 and 0.″7 (FWHM).

Five 120s images were made in the *J* band on 1991 October 1, and eleven 60s images were made in the *K* band on 1991 September 30. The object was placed in various positions on the array. The sky level at each pixel was taken to be the median value of the images. Imaging photopolarimetry observations were made in the H band on 1991 September 29 using a rotatable half wave plate and a linear polarizer directly in front of the dewar window. Three 120s images were made at each of four different position angles of the half wave plate. Following flattening and sky subtraction the images were shifted and medianed to produce the final *J, H,* and *K* images shown in Figure 1 (Plate ?). Only the central region surrounding MG 0414+05340414 that was observed in all the frames is shown.

The photometric state was determined by observations of several standard stars from Elias *et* al. (1982). The brightness of the individual components was determined by summing the signal in apertures with diameters of 4 pixels (1.″6) centered on the image peaks. Photometric uncertainties are dominated by the aperture corrections determined from the observations of standard stars. Results are given in Table 1.

Neither the lensing galaxy nor what Schechter and Moore (1992) called '(object x" was detected. Schechter and Moore used point-spread-function (PSF) fitting to disentangle the overlapping components of MG 0414+05340414 in images taken in moderate seeing, and thereby detect extended emission of low surface brightness that they identified with the lensing galaxy. Unfortunately, there were no objects in the small field of our infrared images that could be used to construct a reliable PSF. In any case, profiles through various parts of the image gave no indication that a lensing galaxy had been detected. This is not surprising.

FIG I.---a) Combination of five 120s images in the J band. North is at the top, east is to the left. The maximum separation of the components i.. 2.″15. b) Combination of twelve 120s images in the H band. c) Combination of eleven 60s images in the K band. From brightest to faintest the images are A1+A2, B, and C. Al and A2 are separated by 0.″4 (Al is almost directly south of A2) and are unresolved here.

Schechter and Moore determined an I magnitude for the lens of 23.36 msg. Typical $I-K$ colors of galaxies at redshifts of 0.5 are 1.5-2.5 msg. Thus in the K band we expect the lens to contribute $\lesssim 0.1\%$ of the total light.

The K-band image taken by Annis and Lupino (1993) with a 256 x 256 array goes significantly deeper than ours, as well as covering a much larger field. Our images provide no useful information about the nearby objects seen by Annis and Lupine, which may be important in lensing models.

The polarization data were analyzed by the method of Elston and Jannuzi (1995) using reflection nebulae to calibrate the position angle of any observed polarized emission, We obtain a fractional polarization p in the H band of $0.4 \pm 1.0\%$, uncorrected for statistical bias (i.e., polarization is positive definite, so at small values measurement uncertainties bias the result upward [Wardle & Kronberg 1974]). MG 0414, therefore, was not highly (or significantly) polarized. Local interstellar polarization was not determined from field stars, but is probably less than a few tenths of a percent in the near infrared at such high galactic latitude.

3. HIGH RESO1,UTION IMAGING

MG 0414+0454 was observed with HST on 1991 Nov 3. Exposures of 500 and 1000 s were made through the 702W filter. The images were debiased and flattened in the STScI pipeline. Cosmic rays were removed with the STSDAS routine CRREJ.

The pixel size was 0.″043. No absolute photometric calibration was attempted. Relative fluxes of A], A2, B, and C were determined both by aperture photometry with several different apertures and by fitting Gaussians to the cores of the images. The large uncertainties in the values given in Table 2 were determined from the scatter in the results obtained by the various methods, and are due to the combined effects of extended and strong wings in the early HST PSF and the low signal-to-noise ratio of the image.

Another consequence of the low SNR is that the image contains no information about either the lens or Schechter and Moore's '(object z." The lensing galaxy in the fits of Schechter and Moore (1992) is 0.3 mag brighter than C in the I band, but its light would be spread over thousands of pixels in the HST image and would be undetectable unless it was highly nonuniform. Similarly, object x is 1.5 mag fainter than C in the I band. Even if it were unresolved (e.g., a foreground star) it would be undetectable in the HST image.

4. FAR INFRARED PHOTOMETRY

IRAS scans at the position of MG 0414-t 0454 were examined with the IPAC SCANPI procedure. Noise levels of 18, 24, 40, and 262 mJy were obtained in the scan medians at 12, 25, 60, and 100 pm, respectively. Nothing was detected above the noise at 12 and 100 μm. At 60pm a flux density of 180 $\pm$ 38 mJy was found centered 2" (1/50th of a beam) from the nominal position of Al +A2, while at 25 μm a marginally significant flux density of 70+ 20mJy was found 4" (1/10th of a beam) from the nominal position.

The overall spectral index of MG 0414+0454 (including the lens) between 60 and 2.2 μmis –1.32 ($S \propto \nu^{\alpha}$). If the marginal 25pm detection is real, the overall spectral index between 60 and 25 μm is – 1.08. For either of these values, the non-detections at 12pm and 100 μm are no surprise, given the noise levels in the IRAS data.

Table 1 summarizes the photometry results from this work, along with measurements by others. Table 2 gives the flux ratios of various components, which vary widely with frequency. Flux-ratio differences in lensing, which is achromatic, are usually explained with

appeals to variability (combined with time-delays and non-simultaneous measurements), or to the different sizes and locations of the emission regions at different frequencies. Neither explanation seems plausible in the case of MG 0414+0454. We will return to this important topic in § 9.

TABLE 1

ABSORPTION FEATURES OF MG 0414+0534 A and B

Name	Center (A)	Ampl. (μJy)	FWHM (A)	W_{obs} (A)
A				
Fe II λ2343.495	8511.32	–13.1	3,6	1.5
	8518,70	-26,6	4.0	3.4
	8537.01	-11.9	3.5	1.3
	8541.83	–14.5	2.5	1.2
Fe II λ2373.737	8621.12	-6.4	2.4	0.5
	8628,60	–24.6	2.4	1.8
	8647.14	–5.5	2.0	0.3
	8652.03	–5.5	2.0	0.3
Fe II λ2382.039	8651.34	–23.6	3.2	2.2
	8658.84	–30.2	5.2	4.7
	8677.45	–23.3	2.'7	1.9
	8682.35	–24.6	2.7	2.0
B				
Fe II λ2343.495	8511,87	–5.0	2.0	1.2
	8518.59	–7.3	3.8	3.3
	8537.74	–4,9	2.2	1.2
	8542.05	–4.0	3.1	1.4
Fe II λ2373.737	8621.68	-1.7	4.2	0.8
	8628.49	–3.5	2.4	0.9
	8647.88	–0.6	2.0	0.1
	8652.24	–0.6	2.0	0.1
Fe II λ2382.039	8651.89	–6,6	3.6	2.5
	8658.73	-7.0	4.6	3.4
	8678.19	–4.6	3.0	1.4
	8682,57	–7.7	2.4	1.9

5. INFRARED SPECTROSCOPY

Near-infrared spectra were obtained with the KPNO *CRSP* infrared spectrometer at the $f/30$ focus of the 4 m telescope on 1991 October 17 and 18. The *CRSP* has a 58 x 62 InSb array. Observations were made using the multiple correlated sampling technique described by Fowler and Gatley (1990), which gives a read noise of $\sim$ 90 electrons.

A *751* mm^{-1} grating and a 510 μm (2.″5) slit gave resolutions of 140 in the J band (4th order), 130 in the H band (3rd order), and 110 in the K band (2nd order). The 25'' -long slit was oriented east-west. Each band can be covered with only one setting of the grating. A series of 1 minute exposures was made in each band, with the object moved about 10' along the slit between exposures. The nearby (< 10°) star BS 1279 was observed before and after each series to locate the center of the slit relative to the offset guider and to remove telluric absorption and instrumental throughput variations.

TABLE 2

RATIOS OF COMPONENTS OF MG 0414+0534

Band or Frequency[a]	A1/A2	A/B	C/B	Date
5 GHz [b]		5.09 ± 0,05	0.36 ± 0,01	1984 Dec 17
8 GHz [c]	1.11 ± 0.01	4.99 ± 0.03	0.42 ± 0.01	1990 Apr 2
15 GHz [b]		4.98 ± 0.05	0.37 ± 0.01	1987 Dec 22
15 GHz [c]	1.16 ± 0,04	5.09 ± 0.08	0.41 ± 0.02	1990 Apr 2
15 GHz [d]	1.13 ± 0.07	4,88 ± 0.26	0.37 ± 0,03	
K (2.188 pm)		4.13 ± 0.18	0.54 ± 0.04	1991 Sep 30
K′ (2.11 μm) [e]		3,90 ± 0.20	0.59 ± 0.03	1991 Dec 18
H (1.644 μm)		3.73 ± 0.17	0.53 * 0.04	1991 Sep 29
J (1.251 pm)		2.92 ± 0.13	0.59 ± 0.05	1991 Ott 1
z (0.884 μm) [b]		2.91 ± 0.11	1.03 ± 0,17	1988 Feb 16
I (0.806 μm) [b]		2.88 ± 0.08	0.68 ± 0.04	1987 Sep 29
I′ [f]	2.51 ± 0,18	3.16 ± 0.07	0.49 * 0.3	1991 Nov 3
I [d],	3.3 * 1.1	3.2 ± 0.2	0.4 ± 0.1	1992 Mar 1 1992 Sep 25
702W (0.715pm)	2.43 ± 0.47	2.58 ± 0.26	0.42 ± 0.08	1991 Nov 3
r (0.662 μm) [b]		2.58 ± 0.26	1.04 ± 0.13	1988 Feb 16
R (0.647 μm) [b]		1,87 ± 0.10	0.73 * 0,07	1987 Sep 29 1989 Ott 27

Notes to TABLE 2

[a] Wavelengths for bands are centroids; see Table 1 for ranges,
[b] Hewitt *et al.* (1992), with errors from Katz and Hewitt (1992)
[c] Katz and Hewitt (1992)
[d] Katz, Hewitt, and McMahon (1994)
[e] Annis & Luppino (1993)
[f] Schechter and Moore (1992). The lens and the images were separated by simultaneous fitting.
[g] Angonin-Willaime *etal.* (1994a, 1994 b). The lens and the images were separated by PSF and Gaussian fits.

Dark current and night sky emission were removed by subtracting adjacent spectra. After division by a dome flat, sky variability was removed by fitting and subtracting a low order polynomial across the dispersion. Twenty exposures were made in *J* and ten each were made in *H* and *K*. The spectra were shifted and combined by taking the median value for each pixel before optimal extraction, The wavelength scale was determined from unresolved emission and absorption features in the night sky, with rms residuals of 0.5 pixels (0.0022 μm, 0.0029 μm and 0.0044pm at *J, H,* and *K* respectively). The spectra were corrected for atmospheric absorption and the instrumental response assuming that BS 1279 is a 6300 K black body in the near infrared. The result is shown in Figure 2a.

MG 0414+0454 was too faint to be seen directly in the guider, and there was no bright star of known position (i.e., an HST guide star) within the guider travel range around the position of MG 0414+0454. The less accurate offset pointing of the telescope itself was used to put MG 0414+0454 in the slit. Centering errors lead directly to uncertainty in both the absolute and the relative flux levels of the three spectra.

To confirm the KPNO *CRSP* spectra and to better define the overall shape of the infrared spectral energy distribution of MG 0414+0454, we obtained a second set of spectra using the *OSIRIS* imager/spectrometer on the CTIO 4 m telescope on 1993 September 22

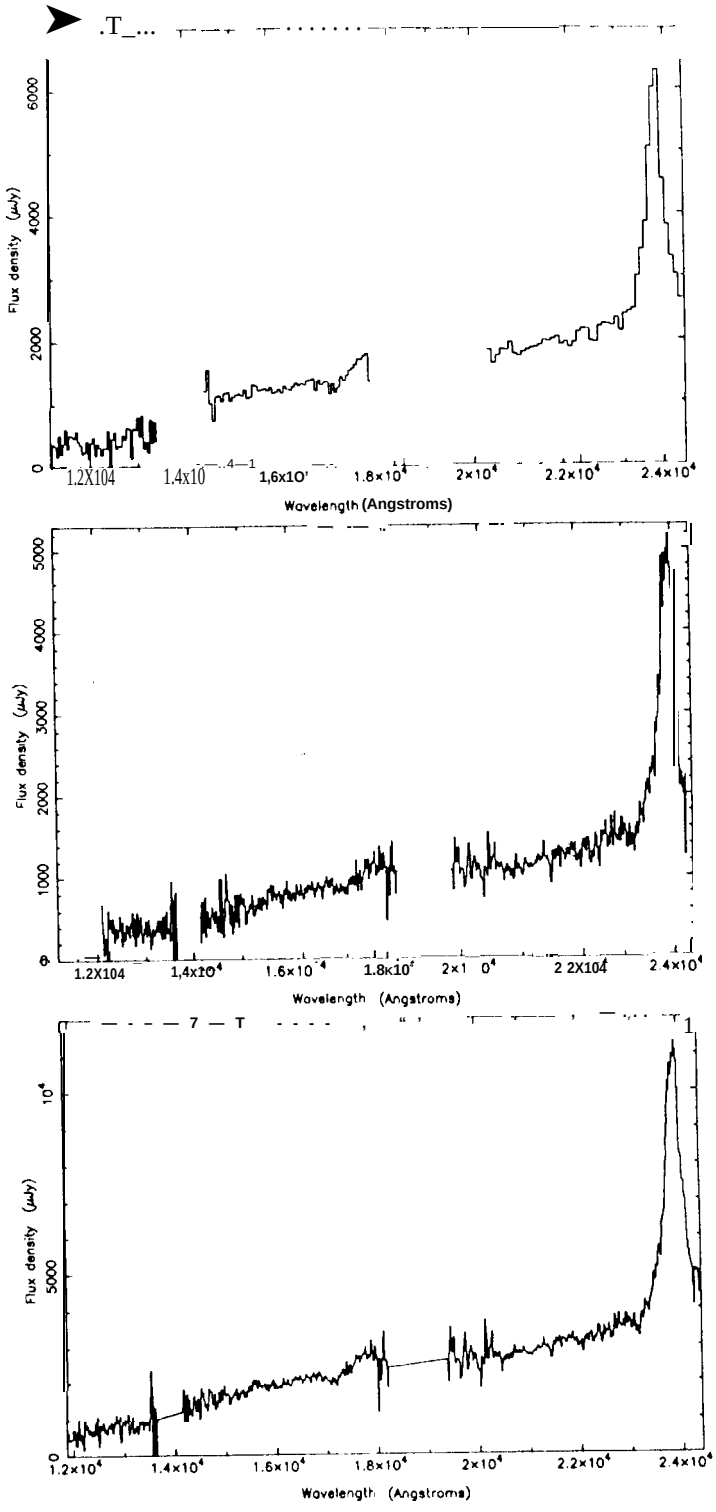

FIG 2.— Near-infrared spectra of MG 0414+0454. a) Spectrum taken with the *CRSP* spectrograph on the KPNO 4 m telescope. b) Spectrum taken with the OSIRIS spectrograph on the CTIO 4 m telescope. c) Combined spectrum, adjusted to match the broadband photometry of Table 1 (see text for details).

and *23. OSIRIS* uses a *256 x 256* HgCdTe NICMOS 3 array produced by Rockwell, which has a read noise of 30 electrons when used with double correlated sampling. A cross-dispersing grism was used to separate the orders, allowing the *J*, *H*, and *K* bands to be observed simultaneously in the 5th, 4th, and 3rd orders, respectively. A 1.″2 slit, f/2.8 camera, and a 1501 mm^{-1} grating blazed at 6.5 μm gave a resolution of 550 and an array scale of 0.″45 pixel^{-1} along the slit. Component A was centered in the east-west slit using OSIRIS in its imaging mode. A total of 12 exposures was obtained through thin cirrus; each exposure was the sum of three 60s integrations. The source was moved along the slit between exposures. The illumination of the array by the cross-dispersed spectra is such that for some positions of the object along the slit wavelengths longer than 2,35pm fall off the array. The bright A2V star HR1 522 was observed for calibration.

The data were reduced similarly to the *CRSP* data, except that the higher resolution allows a more accurate determination of the wavelength scale. Fits to about 70 night sky emission lines gave RMS residuals of 0.15 pixels (1.8 Å, 2.1 Å, and 2.9 Å at *J*, *H*, and *K* respectivel y). The spectra were corrected for atmospheric absorption and the instrumental response assuming that HR 1522 is a 9120 K black **body** in the near infrared. Absolute flux density levels were based on the expected $V - K = 0.13$ mag color of an A 2V star and photometry given for HR 1522 in the Bright Star Catalogue. Since conditions were not photometric, and the spectra were obtained through a narrow slit, the absolute flux density calibration of the OSIRIS spectra is uncertain. Nevertheless, since thin cirrus is grey, differential atmospheric refraction is small in the near-infrared, and all three bands were observed simultaneously, the *relative* flux density calibration of the *OSIRIS* spectra should be excellent for wavelengths less than 2.35 microns. Beyond 2.35 μm, where the image of part of the slit falls off the array, MG 0414-t 0534 was not observed in many of the exposures, and the calibration becomes more uncertain. The result is shown in Figure 2b.

The two sets of spectra agree in their basic features, the most remarkable of which is the imposing emission line centered near 2.3 pm. Before they can be combined, however, several differences must be taken into account.

The first difference is in the wavelength calibration. The strong emission line is well-fitted by a Lorentzian profile centered at 2.3800 μm in the *CRSP* spectrum and 2,3885pm in the *OSIRIS* spectrum. The 79..5 Å difference in centers is less than twice the uncertainty in the *CRSP* wavelength calibration, and corresponds to 0.5 resolution elements (0.9 pixels) in the *CRSP* spectrum. Since the the higher resolution *OSIRIS* spectrum has much smaller wavelength uncertainties, we simply shifted the *CRSP* spectrum redward until the line centers were equal.

The second difference is in the absolute flux density levels of the two spectra. This is not unexpected, given the different slit widths, atmospheric conditions, and epochs for the observations, Correction factors were calculated by comparing the integrated flux of the *CRSP* and *OSIRIS* spectra with that of a constant 2012 μJy spectrum over the H-filter band pass (see Table 1). The *H* band was chosen because the spectra have a higher signal-to-noise ratio there than in the *J* band, and because the strong emission line at the edge of the *K* band makes the *K* band result sensitive to the exact filter bandpass. Analytic functions fitted to the continuum were used to extend the *CRSP* spectra into the atmospheric gaps, so that the entire range of the *H* filter was covered. The derived correction factors for the *CRSP* and *OSIRIS* spectra were 1.58 and 2.44, respectively, and adjust the spectra to the integrated level of the *entire system.* Although this procedure ignores the different colors of A, B, and C (see Table 2) and their differing relative contributions to the two sets of spectra (the effect of different slit widths, pointing errors, and seeing), A is so much brighter than

B and C that this is relatively unimportant.

Finally, because the two sets of spectra differ in spectral resolution and wavelength coverage, the following steps were taken to combine them: 1) both sets of spectra were rebinned to an increment of 12.5 Å pixel^{-1}; 2) analytic functions were fit to lines and continuum; 3) the analytic functions were averaged; and 4) the residuals after subtraction of the analytic functions were either averaged (where the spectra overlapped) or copied from the single spectrum. Finally, the averaged residuals were added back to the averaged analytic functions. The result of all of the steps described above is shown in Figure 2c.

6. THE OVERALL OPTICAL/INFRARED SPECTRUM

MG 0414+0534's exceptionally red continuum in the range 4300–9800 Å (Hewitt *et al.* 1992) is unique among extragalactic radio sources. The new infrared spectra increase by almost a factor of 2.5 the range of wavelengths that has been observed spectroscopically y in this source. In the previous section the absolute level of the infrared spectrum was adjusted to match the H-band photometry. Before the optical and infrared spectra can be combined, the absolute level of the optical spectrum must be established in a similar way.

The best band to use for this is the I band, both because the spectrum has the highest SNR there and because the l-band measurements of Schechter and Moore (1992, see Table 1) were made only a month after the H-band measurements. The relative calibration of the optical and infrared spectra then has three significant uncertainties. First, the variability of MG 0414+0534 is unknown, and core-dominated radio sources sometimes. vary significantly in a month. Second, the fraction of the total emission coming from the galaxy is likely to be much higher in the I band than in the H band, as galaxies are significantly bluer than MG 0414+0534. The fits of Schechter and Moore (1992, their Table 2) allow the galaxy to be subtracted out, at the cost of increased uncertainty. Third, as discussed in Schechter and Moore, the extreme difference between the colors of MG 04 14+0534 and standard stars in the I band makes photometric calibration tricky. From the spectrum itself we can determine $V - I = 3.7$ mag, which according to Schechter and Moore would give an 0.08 mag offset between their observed magnitudes and standard I magnitudes. We decided that inclusion of such a color term, which has its own uncertainty, would not increase our confidence in the result. Ignoring it, we derived a correction factor for the optical spectrum of 2.51. We would not be surprised if the relative levels of the optical and the infrared spectra are off by 20'% or so. The combined optical and infrared spectrum is shown in Figure 3.

7. THE REDSHIFT OF THE RADIO SOURCE

The line near 2.4 μm has a FWHM in excess of 300 Å, equivalent width of about 1000 Å, and line-to-continuum ratio approaching 2. Identification of this line as H α at $z = 2.639 \pm 0.002$ is confirmed by the feature at the edge of the H-band spectrum, the expected location of H β (see § 9.1 for details). A weak line is seen where H γ should appear. The weakness of Hγ is not unexpected given the large ratio of H α to H β. Two lines usually seen in quasars, [0111]~4959, [0 II] λ3727, fall at the edges of the observed J- and H-band *OSIRIS* spectra. Neither was detected. Given the low signal-to-noise ratio, and the fact that both lines tend to have rather low line-to-continuum ratios in quasars, this is not surprising. The center of a much more prominent quasar line, Mg II λ2800, would fall in the gap between the optical and the infrared spectra. 'I'he mean value of the spectrum from 1209-1225 Å (Ly α), is 0.3+ 1.0 μJy, while from 1537-1560 Å (C IV λ1549) it is 0.5+ 0.7 μJy. In neither case is line or continuum emission detected. However, a weak Lorentzian with the same

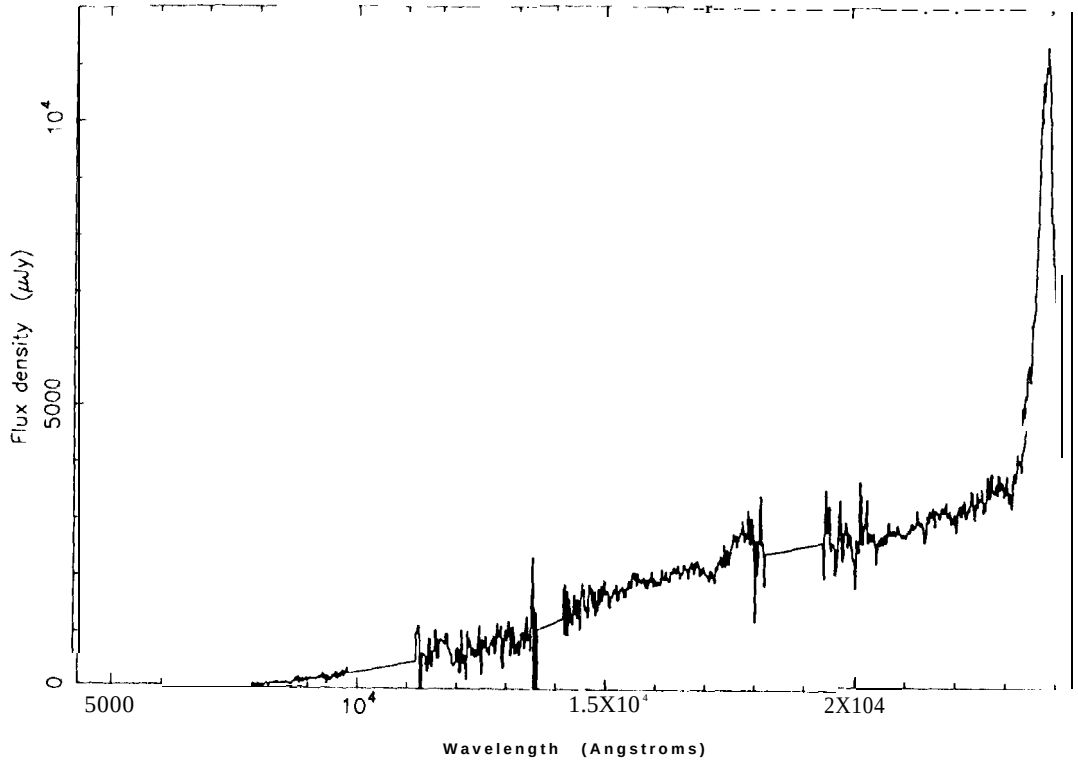

FIG 3---- Spectrum of MG 0414+0534 from 0.43-24pm. The optical spectrum (from Hewitt *et al.* 1992) has been multiplied by 2.51 to match the broadband photometry of Schechter and Moore (1992, see text), The infrared spectrum is the same as in Figure 2c.

velocity width as Ha, fixed at the position of C III]λ1909, follows the spectrum better than a smooth function that fits the continuum alone, and provides a tentative detection of C III]. More detailed consideration of the spectrum, including the remarkable absence of the strong ultraviolet lines, is deferred until § 9, when the nature of the continuum is discussed.

8. THE ABSORPTION FEATURE NEAR 8660 AA

Hewitt *et al.* 1992 did not identify the resolved absorption feature near 8660 Å in their low-resolution 4-Shooter spectrum. On general grounds the most likely identifications are the Mg IIλλ2796.35, 2803.53 doublet, which would have a separation of 22 Å at 8660 Å (z = 2.10), and the Na Iλ5891.58, 5897.56 doublet, which would have a separation of 9 Å at 8660 Å (z = 0.5). Note that an extremely massive lens would be required at z = 2.10.

To make a definitive choice between Mg II and Na I, we observed MG 0414+0534 twice at a resolution of about 4000 with the Low Resolution Imaging Spectrograph (LRIS) on the 10 m Keck telescope, The first observation was made during a very early LRIS engineering run in the fall of 1993. Various electronic problems led to large and non-random readout noise. Nevertheless, a doublet with 9 Å separation was detected at the expected place, which seemed to confirm the identification of Na I at z = 0.47. However, as we report in LCO95,

a second Keck observation was made in the fall of 1994 after the readout electronics were fixed. The second spectrum has a much higher signal-to-noise ratio than the first, and shows not a doublet with a separation of 9 Å, but a collection of 12 Fe II lines in four sets of triplets at slighly different redshifts quite near the quasar itself. The coincidental separation of the two strongest features by roughly 9 Å explains why the noisy first Keck spectrum apparently confirmed an erroneous identification of the absorption "feature" with Na I.

As discussed in LC095, the strength of the iron absorption in MG 0414+0534 is unusual, but not unprecedented. Unfortunately, the redshift of the lens itself remains unknown.

9. DUST

Any one of three characteristics of MG0414+ 0454 would put it sufficiently outside the range of normal properties of quasars, galaxies, and lensing to require explanation. These are: 1) the unique optical/infrared spectrum; 2) the different broadband colors of the components; and 3) the large 60pm flux density (compared to the observed optical/near infrared flux density).

It is conceivable that these characteristics all have origins unrelated to each other or to lensing. In this section, however, we argue that there is a single, lensing-related explanation for them all, namely, an extremely dusty lensing galaxy.

9.1. *Dust y lens vs. dusty quasar- -overview*

We begin with a summary of why we believe that dust in the lens, not dust in the quasar or simply an intrinsically red quasar, explains the extremely red colors of MG 0414+0534. There are three reasons:

1. The observed optical/infrared spectrum of MG 0414+0534 can be fitted very well by standard quasar "components" suitably reddened by dust at z = 0.5, the "most likely" redshift calculated theoretically by Kochanek (1992). Dust at z = 2.64 with ultraviolet extinction as observed in the Small Magellanic Cloud (i. e., no 2200 Å feature) gives a significantly poorer fit. Dust at z = 2.64 with standard Galactic ultraviolet extinction is hopelessly bad.

2. The images have different colors, which can be explained easily by differences in extinction along paths through the lens separated by up to 10 kpc. The separation of the paths inside the host galaxy of the quasar is much less than a parsec, however, and a different explanation would have to be found for the different colors of the images.

3. The quasars in MG 0414+0534 and MG 1131+0456 are the reddest quasars known to us. It is possible that these red objects both just happen to lie behind intervening galaxies without the galaxies having anything to do with the red colors. It is much more likely that the quasars are red *because* they lie behind galaxies.

9.2. *The shape of the* spectrum

Figure 4 shows the spectrum ofMG0414 -+-0534 at rest wavelength. The smooth curves are various components fitted to the spectrum. The Lorentzians that fit HP, H γ, and C III] λ1909 are fixed to have the same velocity width as Ha. 'I'heir centers are tied to that of H α as well.

Our model for the continuum is a flat spectrum (i.e., $F_\nu \propto \nu^0$) extincted by dust at z= 0.5 with A_v = 5.5 mag. The amplitude is adjusted for best fit to the spectrum of MG 0414+0534. We used the extinction law of Cardelli, Clayton, and Mathis (1989) above 5494 Å in the rest frame of the dust (i.e., the *V* band), and the SMC extinction law of Prévot et *al.* (1984) below 5494 Å. The Prévot *et al.* law is adjusted to match that of Cardelli *et al.*

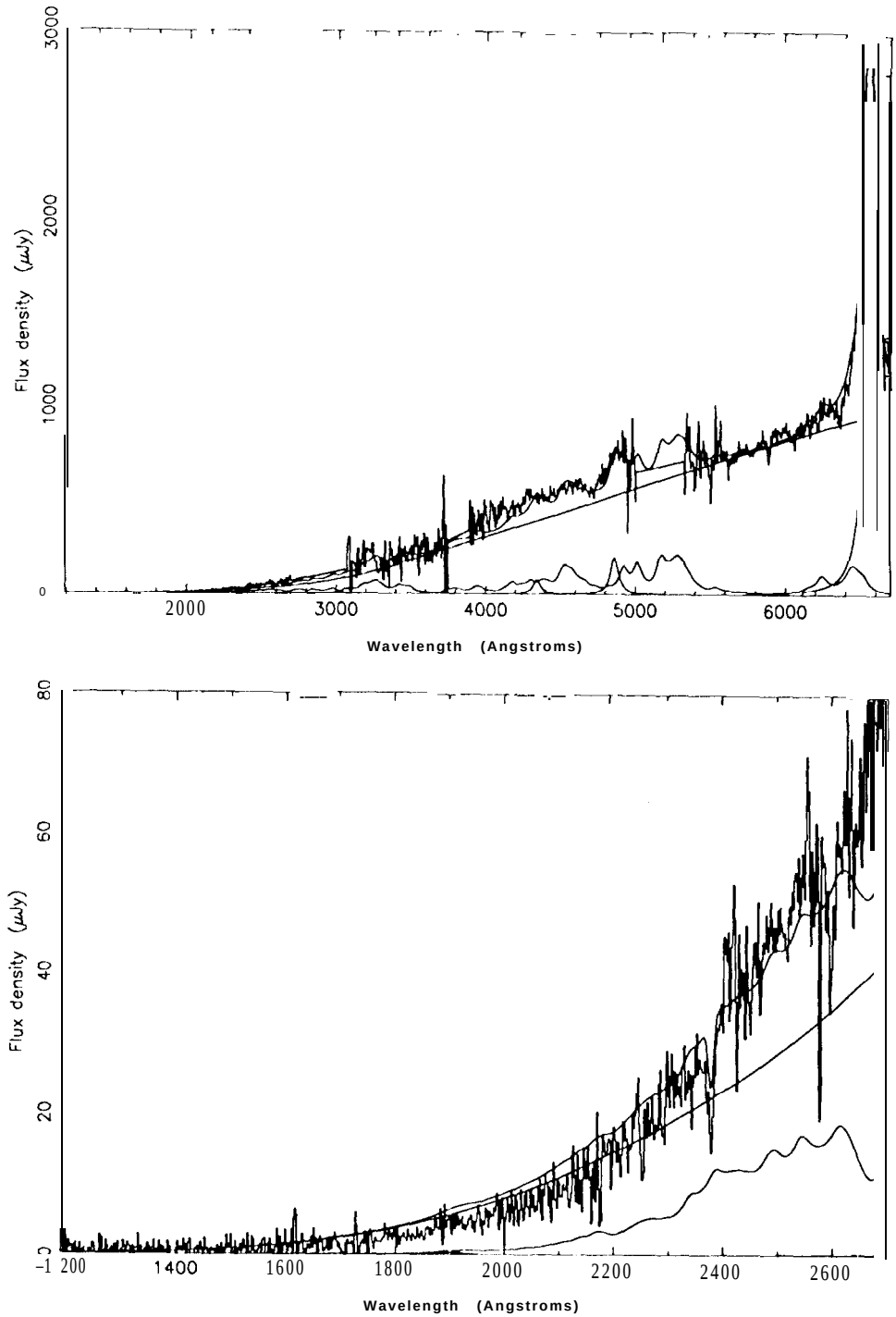

FIG 4.— Combined optical and infrared spectrum of MG 0414, at the rest wavelength of the 2 = 2.639 lensed quasar. The top panel shows the entire spectrum, while the bottom panel shows the observed wavelength range 4309700 A enlarged for clarity, The smooth lines are functions fitted to the spectrum, and include: 1) an $F_\nu \propto \nu^0$ continuum reddened by dust at z $\approx$ 0.5 with ..4$_v$ = 5,5 mag and $R_v = 3.1$; 2) individual lines, most notably Ha, H L?, and Hγ; and 3) a large number of Fe II lines, convolved with a Lorentzian of velocity width 4300 km s^{-1}, reddened the same as the continuum, and fitted in three pieces. The sum of all these functions is also shown. Parameters for individual lines are given in Table 3.

at $\lambda = 5494$ Å. We used the "normal" galactic ratio of $R \equiv A_V/E(B-V) = 3.1$ (Cardelli *et al.* 1989). Although the SMC law, with no 2175 Å feature, is smoother than the Cardelli *et* al. law, for dust at $z = 0.5$ the differences between the two extinction laws over our observed wavelength range are small.

In addition to the reddened continuum and the obvious emission lines, the spectrum shows evidence for strong Fe II emission. This evidence is strongest near H α and H β, where asymmetries or deviations from a smooth Lorentzian profile are characteristic of iron emission. We used model iron spectra from Wills, Netzer, and Wills (1985, kindly provided by B. Wills), convolved with a Lorentzian with velocity width (FWHM) of about 4300 kms-^{1} (close to that of H α), and reddened by the same extinction as the continuum. The iron was fitted independently in three pieces: $\lesssim$3000 Å, 3000–4000 Å, and $\gtrsim$4000 Å. Convolution of the iron with a line profile broader than that of H α would improve the fit in several places by smoothing out the wiggles in the iron spectrum, but there is no particular justification for doing so. Templates based on iron emission at low redshift may simply be inappropriate for the strong iron emission seen in MG 0414+-0534 and other luminous high redshift quasars (Elston, Hill, & Thompson 1994). Details of the fits are given in Table 3.

TABLE 3

REST-FRAME EMISSION LINES OF MG 0414+0534, z = 2.639

Name	Type[a]	Center (A)	Ampl. (μJy)	FWHM (A)	W_λ (A)	log *Lb* (W sr^{-1})
HO.	L	6562.9	2092.2	89.9	277	37.79
Na D[c]	G	5886.1	–105.7	14.9	–2.1	
Hβ	L[d]	4S61.4	197.2	66.6[d]	32	36.90
H-y, ...	L[d]	4340.5	79.9	59.4[d]	15	36.55
CIII 1909	L[d]	1909.0	0.3	46.5	[d] 23	34.62

Notes to TABLE 3

[a] L—Lorentzian profile; G—Gaussian profile.

[b] $H_0 = 75\,\mathrm{km\,s^{-1}\,Mpc^{-1}}$, $q_0 = 0.1$.

[c] Narrow feature seen only in *OSIRIS* spectrum. This coincides with no strong atmospheric or instrumental features; however, the *CSRP* spectrum shows nothing, even allowing for the low resolution, and the reality of the feature remains in question. The fitted parameters are based on the average spectrum, giving an amplitude, equivalent width, and luminosity about half se large as in the *OSIRIS* spectrum alone. The redshift of Na I observed at this wavelength would be 2.635, somewhat lower than calculated from H α. It is tempting to associate this feature with the Fe II systems described in §8.

[d] Central Wavelength and width tied to Hα.

It is tempting to associate the difference between observed and fitted emission at the red edge of the optical spectrum to the blue wing of a strong and broad Mg II line (Fig. 4b). To account for the difference, however, the velocity width of the Mg II line would have to be almost three times that of H α. The uncertain relative levels of the optical and infrared spectra, combined with the large atmospheric noise in this part of the spectrum, suggest caution. The question of whether MG 0414+ 0534 has strong Mg II should be decided by future observations that extend the observed wavelength range to 1 μm.

It is clear from Figure 4 that extinction by sufficiently opaque dust in the lens can produce a spectrum like that observed in MG 0414+0534. The low SNR and calibration uncertainties in the observed spectrum, plus the uncertainty in the actual reddening law, make

recovery of the input spectrum by straightforward dereddening impossible. To investigate how well constrained the input spectrum and the amount of reddening are, various input spectra of the form $F_\nu \propto \nu^\alpha$ were assumed, with $-2 \leq \alpha \leq 0$ to cover the usual range in radio quasars. Steeper input spectra required less extinction to produce the sharp drop in the observed optical region. They also required significantly more Fe II to match the overall level of the infrared region, so much, in fact, that the ripples in the iron deviated clearly from the observed spectrum,

The best fit, both qualitatively (i.e., no obvious systematic problems) and in terms of X^2, was obtained with $\alpha = 0$, and with $A_V = 6.0$ mag for the "optical" spectrum and $A_V = 5.0$ mag for the infrared spectrum. The fit given in Figure 4 is a compromise between these two, with $A_v = 5.5$ msg.

An input spectrum with $\alpha = -0.5$ was fitted best with $A_V = 5.0$ mag, while one with $\alpha = -1$ was fitted best with $A_V = 4.5$ msg. As previously mentioned, these steeper input spectra required much more iron emission. For example, the amplitude of the iron near H β was twice as large in the $\alpha = -1$, $A_v = 4.5$ mag case as in the $\alpha = 0$, $A_v = 5.0$ mag case. This led to significant features in the residuals near H α and H β.

Two line ratios, H α/H β and Ly α/H α, provide consistency checks on the estimate of extinction. The 277 Å rest frame equivalent width of the H α emission line is similar to that seen in other high redshift quasars (Soifer *et al. 1981;* Puetter *et al.* 1981; Hill, Thompson, & Elston 1993). The ratio of H α to H β (10.6) is large, with large uncertainty due both to uncertainty in the shape of the continuum and iron emission under the lines and to the fact that the red side of the H α line is not observed. Most quasars at redshifts similar to MG 0414+0454 have ratios in the range 3-5 (Soifer *et* al. 1981, Peutter *et* al. 1981; Hill, Thompson, & Elston 1993), although ratios over 7 (e.g., 1928+738 [Lawrence *et al.* 1995]) have been observed in quasars. For dust at $z = 0.5$, $E(H\beta - H\alpha)/A_V = 0.12$. If the intrinsic ratio of H α/H β lies in the range *3-7,* visual extinction in the range 11–3.7 magnitudes is required to produce the observed ratio. $A_v = 5.5$ mag implies an intrinsic H α/H β ratio of 5.8, within the range for normal quasars.

The non-detection of Ly α in MG 0414+0534 is remarkable. A small amount of dust in the line-emitting region itself would suppress Ly α efficiently because of resonant scattering, but would have little effect on the surrounding continuum. Since the continuum near Ly α is also undetected in MG 0414 +0534, resonant scattering by itself cannot explain the spectrum. Dust at z = 0.5, however, gives $E(\text{Ly}\alpha - \text{H}\alpha)/A_V = 1.8$. The Ly α/H α ratio in the few quasars for which it has been measured ranges from 1 to 3 (Puetter *et al.* 1981, Soifer *et al.* 1981). By fitting a Lorentzian of the same velocity width as the H α line centered at 1216 Å, we find Lyα/Hα < 1 x 10^{-4} in MG 0414+0534. For intrinsic ratios in the range 1–3, this requires visual extinction greater than 5.5- 6.2 magnitudes. Thus extinction from dust in the lens can account simultaneously for the unique continuum shape and the highly unusual line ratios observed in MG 0414+0534.

All fits discussed so far have assumed dust in the lens, Figure 5 shows the spectrum fit with the same components, except that the dust is assumed to be at z = 2.64. Both the SMC and the standard Galactic ultraviolet extinction laws have been fit. As can be, seen the standard Galactic extinction gives a hopelessly bad fit. With the SMC law and an flat input continuum A_V can be adjusted to give a reasonably good fit over the red end of the spectrum, although the model is too high near H α and too low around 4200 Å. But the blue end of the model spectrum is then significantly too high. Moreover, we have not considered the effects of scattering in dust surrounding a quasar, which could raise the blue end even more. The overall match between the red and blue ends of the spectrum is improved with

steeper assumed input spectra; however, the slope across the red end alone then becomes too steep. In our opinion, dust at z = 2.64 cannot reproduce the observed spectrum for any reasonable choice of input spectrum.

9.3. Wavelength-dependent flux ratios

The systematic variation with frequency of the flux ratios given in Table 2 is larger than observed in any other lens system. Lensing itself is achromatic; however, color differences between lensed images can occur if the color of the lensed source varies on time scales comparable to the time delays between images. In general, this would produce scatter in the flux ratios with amplitude dependent on the time between measurements, the intrinsic light curve, and the time delays. Compact radio sources that are variable at optical frequencies are variable at radio frequencies as well, thus in general radio measurements would be affected as well as infrared and optical measurements.

The measurements given in Table 2, made over a period of years, do not show these characteristics. There is little evidence for changes in the radio ratios. And differences in flux ratio increase not with time between observations, but with the difference in frequency. Variability plus time delays (<< 1 year for MG 04 14+0534) would not produce the systematic changes with frequency seen in Table 2.

Differential extinction along the ray paths, however, easily accounts qualitatively for the color differences observed. Quantitative agreement with the present data cannot be expected for two reasons. First, since the measurements at different frequencies were not simultaneous, the just-discussed combination of variability plus time delays may well introduce scatter in the color differences that differential extinction cannot account for.

Second, the lens is extended, and overlaps the quasar images. This has no effect at radio frequencies, because no hint of nuclear activity has been detected in the lens, and non-active galaxies are virtually undectable at high redshifts at radio frequencies. It has almost no effect in the J, H, and K bands either, because the images are so bright compared to the as-yet-undetected galaxy, And it has almost no effect in the high-resolution HST image, because only a tiny fraction of the extended galaxy light would overlap the unresolved quasar images. In optical and near-infrared observations from the ground, however, where the seeing is comparable to the separations of components, the overlap could be significant, especially for the faintest image C. In most cases no attempt was made to account for this overlap. Schechter and Moore (1992) and Angonin-Willaime *et al.* (1994) separated the various components in the I band by fitting PSFs. The fact that the C/B ratios given by Schechter and Moore, Angonin-Willaime *et* al., and our HST image are significantly lower than other measurements at nearby wavelengths supports the notion that contamination from the galaxy affects the measured flux ratios at shorter wavelengths, especially in the very weak C image.

In addition to these shortcomings in the available data, there is the problem that we do not know the redshift of the lens. The dust extinction spectrum is not self-similar at different wavelengths. This allowed us in the previous section to distinguish between dust at z = 0.5 and dust at z = 2.64. On the other hand, the deviation from self-similarity is slow, and we could not, for example, exclude dust at a redshift of 0.6.

In the future, when the redshift of the lens and near-simultaneous photometry in good seeing over a wide frequency range are available, more precise statements can be made about extinction, differential and otherwise. For now the important point is that differential extinction can account quite easily for the very large color differences seen between the various images of MG 0414+0534.

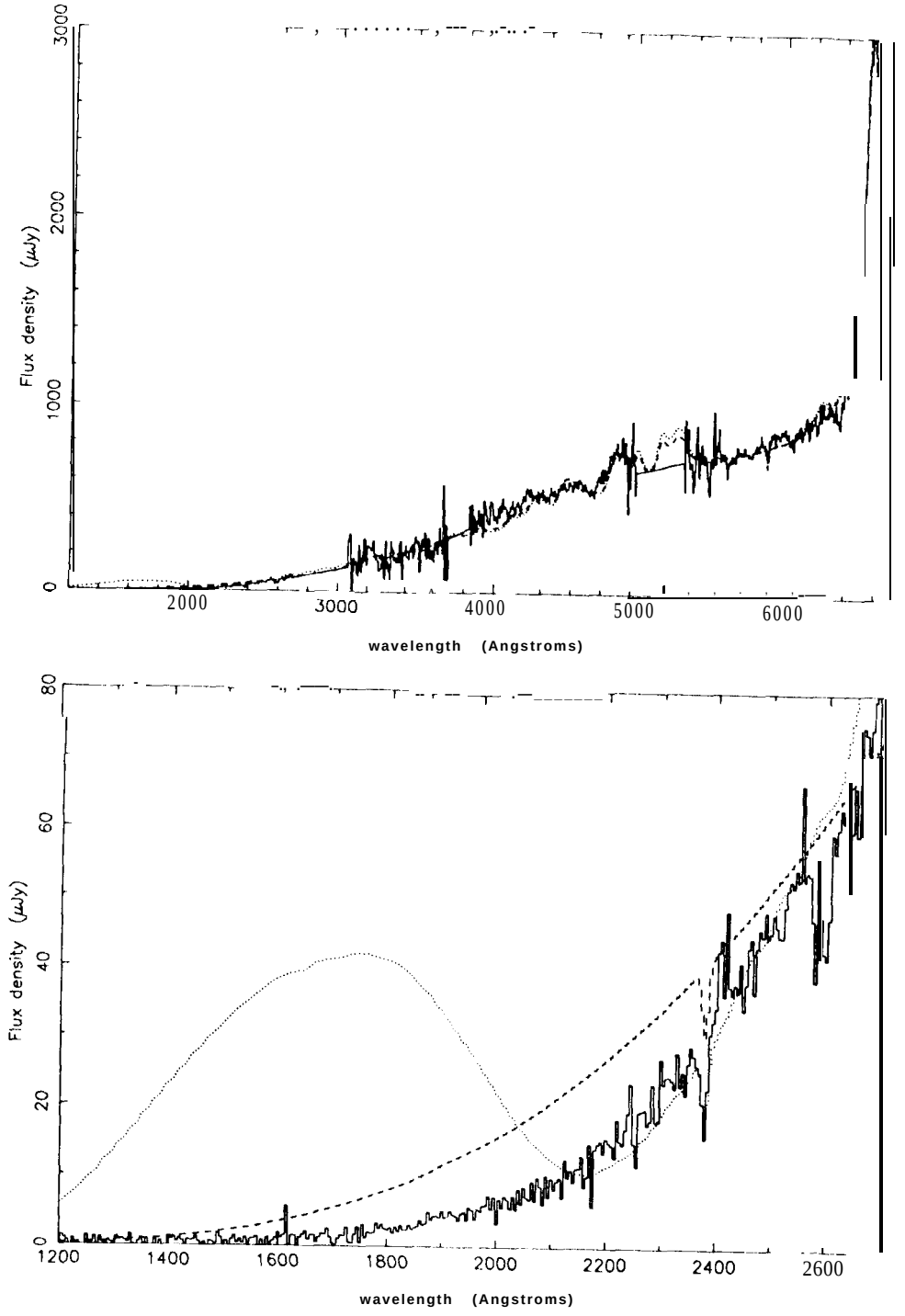

FIG 5--- Same as Figure 4, except that the dust has been placed at the redshift of the quasar. Both "normal" Galactic (Cardelli*et* al. 1989) and SMC (Prévot*et* al. 1984) ultraviolet extinction *were* used. The strong absorption centered at 2175A in the normal law results in a hopelessly bad fit to the observed spectrum. The SMC law does better, but even under the unlikely assumption that there is no Fe

11 in the ultraviolet it cannot match the observed spectrum in both 1400–2600 Å and 3000–4500 Å regions with a single value of extinction,

We begin by assuming a redshift for the dust of 0.5, the theoretically most likely lens redshift, and one that gives an excellent fit to the observed spectrum. Two non-radio measurements of the ratio A 1 /A2 are available, two based on PSF fitting, the other from the HST image. Within the uncertainties these measurements agree, and suggest that the extinction for A2 is about 0.8 mag greater than that for Al (see Figure 6). The A/B ratio given in Table 2 is therefore not independent of A1/A2. As can be seen from the figure, A/B ratios in the infrared bands suggest that *Av* is 0.5--0.8 rnag greater toward A than toward B, while the ratios in the optical bands suggest a difference of 0.2-0.4 msg.

The measured values of C/B cover a wide range. Figure 6 shows only those for which overlap between the quasar images and the lensing galaxy is taken into account. Even these data are not self-consistent at the 1σ level; however, since C/B is the same for the shortest and longest wavelengths observed we conclude that extinction is the same for B and C.

Figure 6 shows that qualitatively differential reddening accounts easily for the wavelength dependence of the flux ratios in MG 0414+0534. The images in order of increasing extinction are (C)B) :Al :A2. (Since A2 at optical and infrared wavelengths is roughly a factor of two fainter than Al, the spectrum in Figure 3 is dominated by Al, and the extinction estimate deter-mined from the spectrum applies roughly to Al alone.) If *Av = 5.5* mag for Al, then for A2 and (B, C) it is about 6.3 rnag and 4.7-5.0 mag, respectively. An accurate determination of the relative reddening along the various image paths must await simultaneous photometry in many bands, accurate separation of galaxy and quasar light, and the redshift of tbe lens.

9.4. *Polarization and* extinction

The maximum observed percent polarization due to dichroic extinction by dust grains along lines of sight in the disk of the Galaxy is correlated with $E(B-V)$. The upper envelope of observed fractional V-band polarizations is given by Aannestad and Purcell (1973) as $p_V^{\max} = 0.09\ E(B-V)$. Assuming a standard Serkowski law for the wavelength dependence of the fractional polarization (Serkowski 1973), and $\lambda_{\max} = 5000$ Å, then dust with $A_v = 5.5$ mag at a redshift of 0.5 would produce a maximum H-band polarization of 5%. The average expected polarization fraction would be roughly half this value, and many factors can lead to little or no polarization even when extinction is large (Goodman *et al.* 1994). Thus the measured value of $p_H = 0.4+ 1.0$'% in MG 0414+0534 is entirely consistent with large extinction.

9.5. Overall energy *spectrum*

Figure 7a shows the overall energy spectrum of MG 0414+0534. The high frequency end falls dramatically compared to that of typical quasars (see, e.g., Sanders *et rd.* 1989). Following correction for 5.5 mag of visual extinction at $z = 0.5$, however, the overall spectrum looks much more normal, albeit noisy. Figure 7b shows the 6700–1200 Å region expanded for clarity. It seems likely that the emission detected by IRAS is almost entirely from the quasar, both because the dereddened energy spectrum looks fairly typical of quasars, and because the amount of dust that we infer from extinction would have to be at a very high temperature to be detectable with IRAS. Definitive statements must await far infrared measurements at high spatial resolution.

Figure 7 provides yet another argument against the idea that the unusual spectrum of MG 0414+0534 is a result of dust in the quasar. Reradiated energy absorbed by dust above 10^{14} Hz would lead to a large far-infrared bump that is not seen.

Integration of the observed spectrum over the optical/infrared region gives a luminosity

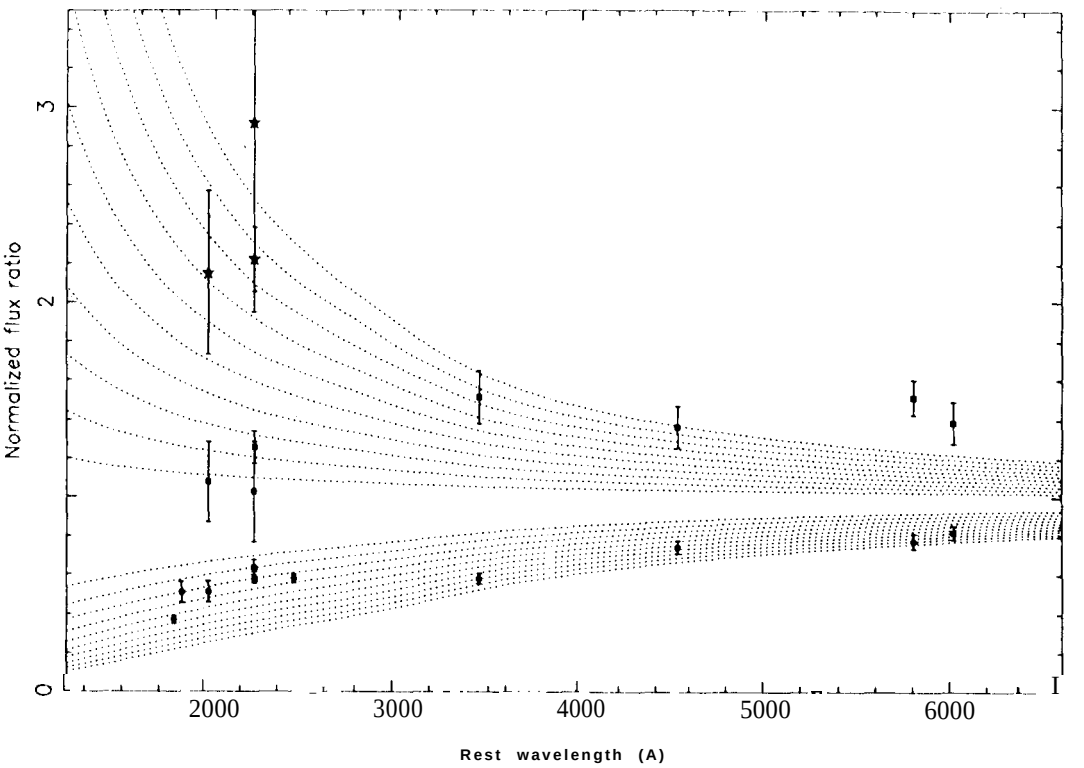

FIG 6.— Predicted effect of differential extinction on flux ratios as a function of emitted wavelength, compared to the observed values. The curves above unity show how the ratios A1/A2 and C/B would change as a function of rest wavelength if extinction to A2 and B was greater than that to Al and C, respectively, by 0.1, 0.2. ... 1.0 mag (the 0.1 mag curves lie closest to unity). The curves below unity show the same for the ratio A/B, once again with 0.1 mag closest to unity. In both cases the curves are normalized to unity at radio wavelengths. Since the variation of A/B with wavelength depends on the differential reddening between A 1 and A2, the lower set of curves must be calculated for a specific value of $A_V^{A2} - A_V^{A1}$, taken here to be 0.8 mag for consistency with the two best measurements of Al /A2. The order of the images from reddest to bluest is A2, Al, (B, C). Measured flux ratios from Table 2 are normalized to the radio ratio, which is unaffected by extinction. A/B measurements are given by filled circles (all < 1); C/B measurements are given by filled squares (all > 1); and A1/A2 measurements are given by open stars. The uncertainties plotted are those given in Table 1, even though they do not take account of important systematic such as variability. Optical and near-infrared measurements of C/B that are likely to be affected by confusing emission from the lens are not plotted. Radio ratios of 5.04 ± 0.03, 0.39 ± 0.03, and 1.13 ± 0.02, respectively, were assumed.

of 1.2 x 10^{39} W sr^{-1}. Dereddening increases this by a factor of over 20 to 2.6 x 10^{40} W sr^{-1}. Even allowing for an overall lensing magnification of roughly a factor of 10, the background source in MG 0414+0534 is thus quite a powerful quasar.

10. DISCUSSION

Significant extinction from dust in the MG 0414+0534 lens can account for: the optical/infrared spectrum of the background source (including the 25 and 60 μm flux densities); the wavelength dependence of the flux ratios of the components; and the unusual H β/H α

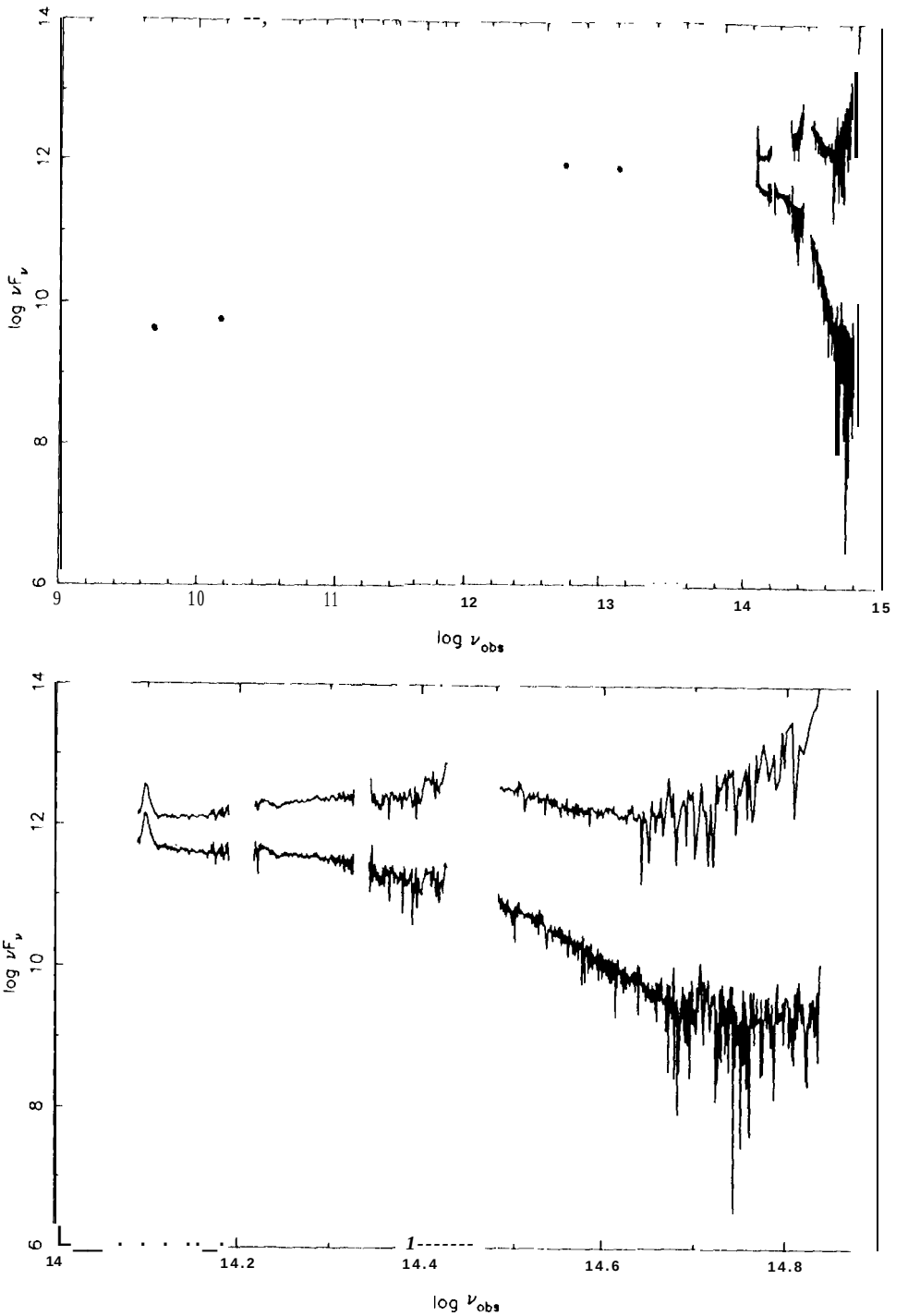

FIG 7.— Overall energy spectrum of MG 0414+0534. The upper curve in the infrared and optical is obtained from the lower by dereddening with $A_v = 5.5$ mag for $R_v = 3.1$ and smoothing. The lower panel gives this spectral *range* expanded for clarity,

and Lyα/Hα ratios. In our opinion, there is no reasonable alternative explanation to dust in the lens, The fact that extremely red images are found in both MG 0414+0534 and MG 1131 +*0456* eliminates whatever small attraction appeals to uniqueness might have had in the individual cases. A consequence of the dust interpretation is that the background source is a powerful, but hardly unusual quasar.

Even large amounts of dust in the lensing galaxy would have little effect *on* its observed colors, although it would be dimmed significantly. This is because the light that is heavily reddened contributes relatively little to the total brightness, and is true whether the dust is uniformly distributed or not, especially when scattering is taken into account as well as absorption. Isolated, dusty galaxies are therefore difficult to identify by their colors alone. The effects of dust in the lensing galaxy on the background source, on the other hand, are dramatic. Gravitational lensing therefore offers a powerful method for identifying and studying dust in galaxies at high redshifts, along multiple lines of sight.

We can make a crude estimate of the mass of neutral hydrogen in the lens as follows, as usual assuming a redshift of *0.5.* Based on the model lens position of Hewitt *et al.* (1992), light from A, B, and C passes within about 6, 6, and 4 kpc, respectively, of the nucleus of the lens ($z_{\rm lens} = 0.5$, $H_0 = 80$, and $0 < q_0 < 1/2$). Crudely speaking, we can say that the extinction at three points on the circumference of a 5-kpc-radius circle is between 4 and 6 msg. Suppose that the extinction is uniform over the entire disk. In the Milky Way, $NH = 5.8 \times 10^{21} E(B-V) = 1.9 \times 10^{21} A_V \, {\rm cm}^{-2} \, {\rm mag}^{-1}$ (e.g., Bolton, Savage, and Drake 1978). This gives NH between 7.5 x 10^{21} and 1.1 x 10^{22} c m^{-2}, corresponding to a total mass of neutral hydrogen inside a circle of radius 5 kpc of about 5 x $10^9 M_\odot$. This estimate, of course, assumes that the relationships between NH, A_v, and $E(B-V)$ are the same in MG 0414+0534 as in the Galaxy, and that the dust is uniformly distributed,

Visual extinction as high as we have found in MG *0414+0534 (4-6* mag) and MG 1131+0456 (3-8 mag, Larkin *et al.* 1994) is rarely found in nearby massive galaxies (see, e.g., Bregman, How, & Roberts 1992; Maoz & Rix 1993). Centaurus A has a dust lane roughly $1' \approx 1.4$ kpc wide extending across the galaxy, with visual extinction between 3.1 and 6 mag (Harding, Jones, & Rogers 1981). The quasar images in MG 1131+0456 could be arranged behind such a dust lane, although optical and infrared images of MG 1131+0456 do not show any such clear feature. The images in MG 0414+0534, however, could not *all* be arranged behind such a dust lane, although they could be covered by something like the 10-kpc-diameter star-forming ring found in the Milky Way and other nearby spiral galaxies, seen face-on.

The possibility that the lenses in MG 0414+0534 and MG 1131+0456 are interacting systems has some appeal. Not only is the only "local" example, Centaurus A, thought to be interacting, but interactions with smaller dust-rich galaxies could inject a lot of dust into a massive potential. The irregular shape of the galaxy in MG 1131+0456, and the large excess of faint nearby objects (Larkin *et al. 1994),* give some support to this idea, but no similar data have been obtained in MG 0414+0534. It is possible, of course, that the "6th component" of MG 0414+0534 possibly detected by Schechter and Moore (1992) and Angonin-Willaime (1994) is a manifestation of an interacting or disturbed lens; however, Angonin-Willaime think it is more likely a Galactic star.

Whether the large extinctions in MG 0414+0534 and MG 1131+0456 simply reflect a higher dust content in massive galaxies at high redshift, or reflect an enhanced frequency of dust-producing interactions involving massive galaxies at high redshift, cannot be decided with existing data, Clearly, however, neither MG 0414+-0534 nor MG 1131+0456 could have been found in any optical lens searches made to date. To estimate the fraction of galaxies

with large extinction, we must consider only radio-selected lens systems, summarized in Table 4. Five of the eleven systems are MG sources, and a sixth, 2016+112, was found in the MG survey, but is slighly below the final flux density cutoff for the MG catalog (Bennett *et al.* 1986). Three of the systems, 0218+357, 1422-t 231, and 1938+6648, were identified in a VLA survey of strong flat spectrum radio sources (Patnaik *et al.* 1992a). The other two, 0957+ 561 and 1830– 211, were found independently. 1 n all cases it was the radio structure alone that called attention to the system. Thus the presence or absence of large extinction in the lens did not cause any large selection bias. Nevertheless, since all radio-selected lens systems were not found by a single, uniformly applied set of criteria, subtle biases cannot be ruled out. For example, systems that are particularly faint are harder to work on, and if the radio structure by itself provides only ambiguous evidence for lensing (e.g., a simple double), it may take quite a long time to do the followup optical or infrared observations. In the case of the MG survey, at least, we can say that there are no undecided cases where the evidence for lensed structure is anywhere near as compelling as the cases in Table 4. In our opinion, therefore, statistics on the incidence of dusty lenses are likely to be affected much more by the small numbers involved than by subtle selection biases.

in Table 4 we have tried to assess whether existing data can or cannot rule out significant extinction in images that lie "in" the lens. Without redshifts, or even good images of some of the lenses, this is somewhat arbitrary. For lack of anything better, we have required only that an image lie within about 2" of the observed or modelled center of the lensing potential. If the ratios of images in the radio and the optical/infrared are the same within the uncertainties, or if the optical spectra of several images show no large differences in continuum shape or line ratios that cannot be attributed to contamination by the lensing galaxy, we conclude that there is no evidence for extinction. It is unlikely that extinctions of a couple of magnitudes would have gone unnoticed, but it is less certain that extinctions of, say, 0.5 mag would have been identified.

The references in Table 4 are to papers (not necessarily unique) that allow an assessment of the radio/infrared/optical image ratios or the spectra. Several cases require explanation. In 0218+357 the image separation is only 0.″3. To date, no optical or infrared images have been published with sufficient resolution to determine a flux ratio. Optical spectra show no evidence for extinction (Browne *et al.* 1993); however, if only one of the images were heavily extincted, it's effect on the spectrum would be small. Thus we can rule out large extinction in at *least one* of the images, but not both. In the case of 1830–211, which lies near the Galactic center, Galactic extinction is probably close to 3 mag (Subrahmanyan *et al.* 1990), and no optical or infrared counterpart has been identified to date (Djorgovski *et al.* 1992). In 2016+112, the third image is faint and hard to see at both radio and optical frequencies (Heflin *et al.* 1991; Schneider *et* al. 1986); however, within large uncertainties the image ratios are consistent with no extinction.

Until a larger number of cases can be decided we hesitate to draw any quantitative conclusions about the incidence of dust in galaxies at "high" (i.e., $z > 0.4$) redshifts. That large extinction is seen in two out of six radio-selected lens systems in which it *could* have been seen strongly suggests, but does not prove, that massive galaxies at high redshift contain much more dust than those nearby. It also shows that by no means all galaxies at high redshift contain a lot of dust. Extinction in MG 0414+0534 and MG 1131+0456 is not the only evidence for dust at high redshift, of course. Quasars with damped Ly α absorbers (e.g., Wolfe 1988) appear to be slightly redder than quasars without damped Ly α systems (Pei, Fall, and Bechtold 1991), and direct detection of dust emission has been claimed in individual objects (McMahon *et al. 1994).* Nor, given the connection between

TABLE 4

RADIO SELECTED LENS SYSTEMS

system	θ[a]	Paths through galaxy[b]	Can deride extinction	Large Extinction[d]	Reference
0218+357	0.″3	2	1[e]	no	Patnaik *et al.* 1992
MG 0414+0534	2.2	4	4	yea	This work
MG 0751+2716	1,0	4	0		Lehár priv. comm.
0957+561	6.1	1	1	no	Lanzetta *et al.* 1993
MG 1131+0456	2.0	2	2	yes	Larkin *et al.* 1994
1422+231	1.3	4	4	no	Lawrence *et* al. 1992
MG1549+3047	1.8	0			Lehár *et al.* 1993
MG 1654+1346	2.1	0		·	Langston *et* al. 1989, 1990
1830–211	1.0	2	0[e]	--	Djorgovski *et al.* 1992
1938+6648	1.0	all	o		Patnaik *et al.* 1993
2016+11 .,	3.4	2	2[e]	no	Lawrence et *al.* 1992

Notea to TABLE 4

[a] Maximum image separation.

[b] Number of images with both radio and optical emission (i.e., not radio rings) that lie within about 2" Of the center of the lens.

[c] Number of paths through the galaxy for which data exist that would show evidence for large extinction.

[d] Large extinction could be shown by: differences in flux ratios of images between radio and optical/infrared measurements; extremely red images (e.g., MG 0414 and MG 1131); or spectral shapes characteristic of extinction (e. g., MG *0414).*

[e] See text.

dust and mass loss from stars, would evolution of the dust content of galaxies be at all surprising. It remains to be seen whether extinctions as large as seen in MG 0414+0534 and MG 1131+0456 are the extremes of a distribution, anomolous, or even the result of a process that produces a lot of dust if it produces any at all.

What is clear is that such large extinctions could introduce strong selection biases in optically selected samples of high redshift objects. Radio samples are therefore essential in establishing the quantitative effects of dust, so long as the optically faint "hard ones" are not ignored. For such purposes samples of lensed objects have two important properties. First, multiple imaging requires a high surface mass density. Therefore lensing samples allow us to study dust in the central regions of massive galaxies. Unlensed samples will show more about the outskirts of leas massive galaxies (e.g., the damped Ly α systems), because of the larger cross sections and number densities involved. Second, lensing provides information along multiple paths through the same potential.

As. previously mentioned, no existing optical lens search would have detected either MG 0414+0534 or MG 1131+0456. Future CCD surveys may be sensitive enough to detect MG 0414+0534, but not (probably) MG1131 -t 0456. An interesting question that cannot yet be answered is the effect of dusty lenses on the statistics of optically selected samples. There arc two competing factors at work. Extinction due to dust in the lens dims the observed quasar images, while magnification by the lens brightens them. The net effect depends on the relationship between mass and dust in galaxies, as well as on the shape of the unlensed luminosity function. If, as suggested by the HST Snapshot Survey results (Maoz *et al.* 1993), the luminosity function for optically selected quasars is very steep at the bright end (Narayan 1994), the effects of dust could have a significant effect on the

relationship between the true and the observed luminosity function.

11. SUMMARY

The redshift of the lensed quasar in MG 0414+0534 is 2.639 ± 0.002, as determined from strong emission lines found in infrared spectra. The unique shape of the optical/infrared spectrum and the large color differences between the four images can be accounted for very well by dust in the lens. If the as-yet-undetermined lens redshift is near the theoretically most probable value of 0.5, visual extinction of ~ 5 mag or more is required along four paths separated by roughly 10 kpc in the lensing galaxy. Dust in the lens is strongly preferred over dust intrinsic to the quasar for three reasons: 1) dust at the quasar redshift cannot produce the observed optical/infrared spectrum for any reasonable input spectrum; 2) the color differences between images are easy to account for by differential extinction in the lens, where the ray paths are widely separated, but not near the quasar, where the paths are very close together; and 3) the two reddest quasars known (MG 0414+0534 and MG 1131+-0456) are both gravitationally lensed, with ray paths through the lensing galaxy, It would be an astonishing coincidence if their strange colors had nothing to do with lensing.

There is thus strong evidence for large amounts of dust in the lensing galaxies of two out of six radio-selected lens systems in which large extinctions could have been seen. This suggests that there are significantly more massive galaxies containing a lot of dust at high redshifts than there are locally, but that by no means all galaxies at high redshift contain a lot of dust. Dust in a galaxy has little effect on the observed colors of the galaxy itself, but can have a dramatic effect on the observed colors of background sources. Gravitational lensing, therefore, will be a powerful tool for investigating dust in the central regions of massive galaxies at high redshift.

It is a pleasure to acknowledge the assistance of X. Huang and J. Dalcanton with the HST images and A. Wehrle and IPAC with the *IRAS* data, and to acknowledge useful conversations with J. Larkin, W. Sargent, T. Soifer, and D. Womble. We thank C. Kochanek, J. Hewitt; J. Ellithorpe, and C. Katz for supplying details of their models or measurements, and J, Hewitt again for useful comments as referee that helped us clarify the presentation. CRL thanks the Institute for Advanced Study, and CRL and ELT thank the Aspen Center for Physics, for their hospitality during periods when some of this work was done. CRL acknowledges support from STScI (GO-2350.03-87A) and the NSF; BTJ acknowledges support from NASA (H F- 1045.01 -93A from STScI); and ELT acknowledges support from NASA (NAGW-2173) and STScI (GO-2350.01-87A). *OSIRIS* has been generously supported by NSF grants to the Ohio State University (AST 90-16112 and AST 92-18449). STScI is operated by AURA under contract with NASA.

REFERENCES

Aannestad, P., & Purcell, E. M., 1973, *ARAA,* 11, 309.
Angonin-Williame, M.C., Vanderriest, C., Hammer, F., *k* Magain, P. 1994a, *AA, 281, 388.*
Angonin-Williame, M. C., Vanderriest, C., Hammer, F., & Magain, P. 1994b, *AA, 292, 722.*
Annis, J. R. & Luppino, G. A. 1993, *ApJL,* 407, L69.
Bennett, C. L., Lawrence, C. R., Hewitt, J. N., Mahoney, J., Langston, G. I., & Burke, B. F. 1986, *ApJS,* 61, 1.
Boksenberg, A., Carswell, R. F., Allen, D.A., Fosbury, R.A. E., Penston, M. V., and Sargent, W. L. W. (1977), *MNRAS,* 178, 451.

Bolton, Savage, & Drake 1978, *ApJ*, 224, 132.
Bregman, J. N., Hogg, D. E., & Roberts, M. S. 1992, ***ApJ, 387, 484.***
Browne, I. W. A., Patnaik, A. R., Walsh, D., & Wilkinson, P. N. 1993, ***MNRAS, 263,*** L32.
Cardelli, J. A., Clayton, G. C., and Mathis, J. S. (1989), *ApJ*, 345, 245,
Coleman, G. D., Wu C.-C., & Weedman, D. W. 1980, ***ApJS, 43, 393.***
Djorgovski, S., Meylan, G., Klemola, A., Thompson, D. J., Weir, W. N., Swarup, G., Rae, A. P., Subrahmanyan, R., & Smette, A. 1992, ***MNRAS, 257,*** 240.
Elston, R., Cornell, M. E. & Lebofsky, M. J. 1985, *ApJ*, **296**, 106,
Elston, Ft., Thompson, K. L., & Hill, G. J. 1994, ***Nature, 367, 250,***
Elston, R. & Jannuzi, B. 1995, ApJL, submitted.
Fowler, A. M. & Gatley, Ian 1990, *ApJL, 953,* L33.
Goodman, A. A., Jones, T. J., Lada, E. A., & Myers, P. C. 1994, in preparation,
Harding, F'., Jones, T. J., & Rogers, A. W. 1981, *ApJ*, 251, 530.
Heflin, M. B., Gorenstein, M. V., Lawrence, C. R., & Burke, B. F. 1991, *ApJ, 378, 519.*
Hewitt, J. N., Turner, E. L., Lawrence, C. R., Schneider, D. P. & Brody, J. P. 1992, *AJ*, 104, 968.
Hill., G. J., Thompson, K. L. & Elston, R., 1993, ApJL, in press.
Johnson, H. L, 1963, in Basic Astronomical Data, ed. Strand, K. A., (University of Chicago Press; Chicago), p. 204.
Katz, C. A. & Hewitt, J. N. (1993), *ApJL, 409, 1,9,*
Katz, C. A., Hewitt, J. N., & McMahon, P. M. (1994), in preparation.
Kochanek, C. S. 1991, *ApJ*, 379, 517.
Kochanek, C. S. 1992, *ApJ, 384,* 1,
Langston, G. I. *et al.* 1989, ***AJ, 97, 1283,***
Langston, G. 1. *et al.* 1990, Nature, 344, 43,
Lanzetta, K. M,, Turnshek, D. A., & Sandoval, J. 1993, ***ApJS, 84,*** 109.
Lawrence, C. R., Neugebauer, G., Weir, N., Matthews, K., & Patnaik, A. R. 1992, **MNRAS, 259,** P5.
Lawrence, C. R., Neugebauer, G., & Matthews, K. 1992, ***AJ, 105, 17.***
Lawrence, C. R., Cohen, J. G., & Oke, J. B. 1994; *AJ*; this volume.
Larkin, J. E., Matthews, K., Lawrence, C. R., Graham, J. R., Harrison, W., Jernigan, G., Lin, S., Nelson, J., Neugebauer, G., Smith, G., Soifer, B. T., & Ziomkowski, C. 1994, *ApJL, 420, L9.*
Lehár, J., Langston, G. I., Silber, A., Lawrence, C. R., & Burke, B. F. 1993, *AJ*, 105, 847.
Loveday, J., Peterson, B. A, Efstathiou, G., & Maddox, S. J. 1992, ***ApJ, 390, 338.***
Maoz, Dan, & Rix, Hans-Walter 1993, ***ApJ, 416, 425,***
Maoz, D., Bahcall, J. N., Schneider, D. P., Doxsey, R., Bahcall, N. A., Lahav, O., & Yanny, B. 1993, ***ApJ, 402, 69.***
McMahon, R. G., Omont, A., Bergeron, J., Kreysa, E., *k* Haslam, C. G, T. 1994, ***MNRAS, 267, L9.***
Narayan, R., & Wellington, S. 1994, in *Gravitational* Lenses in *the* Universe, ed. J, Surdej, D. Plaipont-Care, E. Gosset, S. Refsdal, & M. Remy Liège: University de Liège, p. 217.
Patnaik, A. R., Browne, I. W. A., Wilkinson, P. N., & W'rebel, J. M. 1992a, ***MNRAS, 254, 655.***
Patnaik, A. R., Browne, I. W. A., Walsh, D., Chaffee, F. H., Foltz, C. B. 1992b, ***MNRAS, 259,*** 1P.
Patnaik, A. R., Browne, I. W. A., King, L. J., Muxlow, T. W. B., Walsh, D., *et al.* 1992c, ***MNRAS, 261, 435.***
Patnaik, A., Browne, I., King, L., Muxlow, T., Wafsh, D., Wilkinson, P. 1993, in *Sub-Arcsec* Radio *Astronomy*, ed. R. Booth & R. J. Davis Cambridge: Cambridge Univ. Press, p. 136??.
Pei, Y. C. C., Fall, S. M., & Bechtold, J. 1991, ***ApJ, 378, 6,***
Pettini, M., Smith, L. J., Hunstead, R. W., & King, D. L. 1994, ***ApJ, 426, 79.***
Puetter, R. C., Smith, H. E., Winner, S. P. & Pipher, J. 1,.1981, ***ApJ, 249, 345.***
Rieke, G. H. & Lebofsky, M. J. 1985, ***ApJ, 288, 618.***
Rieke, G. H., Lebofsky, M. J. & Kinman 1979, ***ApJL, 232,*** L151.
Sanders, D. B., Phinney, E. S., Neugebauer, G., Soifer, B. T., & Matthews, K. 1989, ***ApJ, 347, 29.***
Sargent, W. L. W., and Steidel, C. C. (1990), ***ApJ, 359, 1,37.***
Serkowski, K, 1973, in I.A. *U.* Symposium No. 52, ed. J. M. Greenberg and H. C. van De Hulst (Reidel: Dordrecht – Holland), p. 145.
Schechter, P. L. &Moore, C. B. 1992, ***AJ, 105,*** 1.
Schneider, D. P., Gunn, J. E., Turner, E. L., Lawrence, C. R., Hewitt, J. N., Schmidt, M., & Burke, B. F. 1986, AJ, 91, 991.
Seaton, M. J. 1979, ***MNRAS, 187, 73p,***
Soifer, B. T., Neugebauer, G., Oke, J. B., Mathews, K., & Lacy, J. H. 1983, ***ApJ, 265, 18.***
Soifer, B. T., Neugebauer, G., Oke, J. B., & Matthews, K. 1981, ***ApJ, 243, 369.***
Stebbins, J., Huffer, C. M. & Whitford, A. E. 1940, ***ApJ, 91, 20,***
Subrahmanyan, R., Narasimha, D., Rae, P. & Swarup, G. 1990, ***MNRAS, 246, 263.***
Wardle, J. F. C. & Kronberg, P. P. 1974, ***ApJ, 194, 249.***
Wolfe, A. M. 1988, in QSO Absorption Lines, ed. J. C. Blades, D. Turnshek, & C. A. Norman Cambridge: Cambridge University Press, p. 297,